Progress In Electromagnetics Research, PIER 42, 107–130, 2003

NUMERICAL ANALYSIS OF SOME SCATTERING PROBLEMS IN CONTINUOUS RANDOM MEDIUM

H. El-Ocla †

Department of Computer Science
Lakehead University
955 Oliver Road, Thunder Bay, Ontario P7B 5E1, Canada

M. Tateiba

Department of Computer Science and Communication Engineering
Kyushu University, Japan

Abstract—In this paper, we present numerical analysis for the following scattering problems: the radar cross-section, the backscattering enhancement, and the angular correlation function for waves scattered from practical targets embedded in random media. We assume perfect conducting targets with various cross-sections to study the effect of target configuration on the scattering problems. Also, we consider different random media with taking account of incident wave polarization. The scattering waves from conducting targets in random media can be estimated by a numerical method that solves the scattering problem as a boundary value problem. In this method, we use current generator and Green's function to obtain an expression for the scattering waves.

† Also with Department of Microwave, Electronics Research Institute, Giza, Egypt

1. INTRODUCTION

There has been a vested interest among researchers in the study of waves scattered backward through random medium. Random media exhibit several interesting scattering and polarization characteristics, such as backscattering enhancement. Backscattering enhancement phenomena are observed for imaging and scattering from rough surfaces and turbulence. These phenomena have also attracted considerable attention among condensed-matter physicists, resulting in a large number of publications on wave localization in disordered media [1–5]. The problem of electromagnetic-wave scattering from targets is an interesting field that has been studied by many researchers for long decades. At the beginning, this problem was investigated for targets in free space. A lot of methods proposed to formulate the scattering field were presented, examples are in [6–8]. On the other hand, the scattering of electromagnetic-wave from targets embedded in random medium is a subject of great practical and intellectual interest in many situations such as remote sensing, radar applications, and surface physics.

Scattering waves propagating in continuous random media are calculated efficiently by a method that uses a current generator to clarify the medium effects on radar detection [9–14]. This method solves the problem of wave scattered from targets in random media as a boundary value and this technique of solution is important for radar detection of a target of finite size. Also, this method uses two operators: the current generator that transforms the incident wave falling on the target into the surface current and Green's function in the random medium. In earlier investigation [11], numerical results for radar cross-section (RCS) of conducting convex bodies such as circular and elliptic cylinders have elucidated that the spatial coherence length (SCL) of incident waves around target is one of the key parameters for the clarification of random media effects on the RCS.

Later, we considered the targets as conducting cylinders with concave-convex cross-sections and limited sizes less than one

wavelength of waves in free space [12, 13]. It was pointed out that there are some anomalies in the enhancement in RCS (ERCS) of the targets in random media. These anomalies occur when H-polarization of incident wave (H-wave incidence) falls on convex portion of the target. However, these anomalies are absent in case of E-polarization of incident wave (E-wave incidence). We have explained that the interference between the direct and creeping waves results in large increase in backscattering wave intensity that leads to anomalous ERCS. Recently, we extended our study and considered large size targets in different random media [14]. However, this recent study was restricted to E-wave incidence and convex illumination region of concave-convex target. In these studies it was found that the target configuration parameters together with the SCL of the incident wave around the target play a leading role in determination of the RCS of partially convex targets.

To get a satisfactory understanding of the parameters that affect the RCS in random media, we consider the targets size to be about 1.5 wavelength of waves in free space and present numerical analysis for the RCS and ERCS of both concave and convex illumination portions of concave-convex targets. In this regard we assume the linear polarization including E and H-wave incidences with different values of SCLs and target complexity.

Correlations of scattered waves from random media and rough surface have been attracted considerable interest and have stimulated even more intensive research activities in recent years [15, 16]. Experimental studies of the correlation function have been conducted for targets in random media as in reference [17]. Those studies have run the detection measurements on simple convex cylinders only buried in random media and also didn't consider the polarization of incident waves. In this regard, authors wanted to handle the correlation problem numerically and assume different circumstances of targets parameters and incident angle with putting into consideration the polarization of incident waves.

To investigate the angular correlation function (ACF) numerically of waves scattered from practical targets of finite size in random media, one of the authors has analyzed the ACF for circular conducting cylinders [18] and showed the following result. The ACF does not depend on the radius of the circle and depends only on the random medium whose thickness is much larger than the radius. Above result has been shown only to a simple shape target and to an E-wave polarization. To make sure the result, we investigate the ACF for targets with different shapes and parameters in random media with taking account of incident wave polarization.

Here, our aim is to analyze numerically the ACF of waves scattered from conducting targets with different shapes and parameters in random media for E and H-wave incidences. In this case, we point out to that our handling of the angular correlation problem is based on the assumption that incident and scattered waves are not correlated. Therefore, on this assumption, we may express the fourth order moment of Green's functions as the products of the second order moments.

The time factor $\exp(-iwt)$ is assumed and suppressed in the following section.

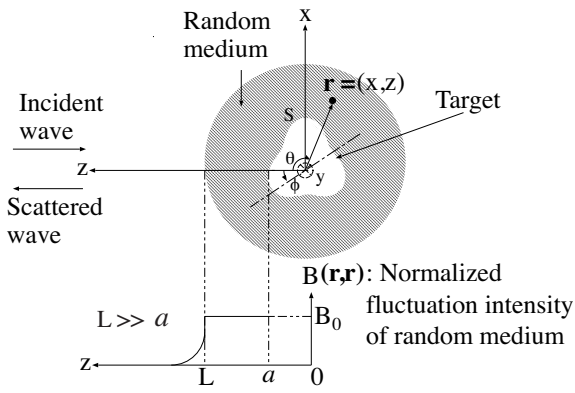

Figure 1. Geometry of the problem of wave scattering from a conducting cylinder in random media.

2. SCATTERING PROBLEM

Geometry of the problem is shown in Figure 1. A random medium is assumed as a sphere of radius L around a target of the mean size $a \ll L$, and also to be described by the dielectric constant $\varepsilon(\mathbf{r})$, the magnetic permeability μ, and the electric conductivity σ. For simplicity $\varepsilon(\mathbf{r})$ is expressed as

$$\varepsilon(\mathbf{r}) = \varepsilon_0[1 + \Delta\varepsilon(\mathbf{r})] \tag{1}$$

where ε_0 is assumed to be constant and equal to free space permittivity and $\Delta\varepsilon(\mathbf{r})$ is a random function with

$$\langle \Delta\varepsilon(\mathbf{r}) \rangle = 0, \qquad \langle \Delta\varepsilon(\mathbf{r})\, \Delta\varepsilon(\mathbf{r}') \rangle = B(\mathbf{r}, \mathbf{r}') \tag{2}$$

and

$$B(\mathbf{r}, \mathbf{r}) \ll 1, \qquad kl(\mathbf{r}) \gg 1 \tag{3}$$

Here, the angular brackets denote the ensemble average and $B(\mathbf{r}, \mathbf{r})$, $l(\mathbf{r})$ are the local intensity and scale-size of the random medium fluctuation, respectively, and where $k = \omega\sqrt{\varepsilon_0\mu_0}$. Also μ and σ are assumed to be constant; $\mu = \mu_0$, $\sigma = 0$.

For practical turbulent media the condition (3) may be satisfied. Therefore, we can assume the forward scattering approximation and the scalar approximation [19]. Consider the case where a directly incident wave is produced by a line source $f(\mathbf{r}')$ distributed uniformly along the y axis. Then, the incident wave is cylindrical and becomes plane approximately around the target because the line source is very far from the target.

Here, let us designate the incident wave by $u_{in}(\mathbf{r})$, the scattered wave by $u_s(\mathbf{r})$, and the total wave by $u(\mathbf{r}) = u_{in}(\mathbf{r}) + u_s(\mathbf{r})$. The targets are assumed conducting cylinders of which cross-sections are expressed by

$$r = ab/\sqrt{(a\sin(\theta - \phi))^2 + (b\cos(\theta - \phi))^2} \tag{4}$$

$$r = a[1 - \delta\ \cos\ 3(\theta - \phi)] \tag{5}$$

Equations (4) and (5) are for convex and partially convex surfaces, respectively, where ϕ is the rotation index. In equation (4), a and b ($< a$) are the half-lengths of the major and minor axes of the elliptic cylinder, respectively. In equation (5), a is the mean size and δ is the concavity index. We can deal with this scattering problem two-dimensionally under the condition (3); therefore, we represent $\mathbf{r}$ as $\mathbf{r} = (x, z)$. According to the polarization of incident waves: E_y or H_y, where E_y, H_y are the y component of electric and magnetic fields, respectively, we can impose two types of boundary condition on wave fields on the cylinder surface S: the Dirichlet condition (DC) for E-wave incidence and the Neumann condition (NC) for H-wave incidence

$$u(\mathbf{r}) = \mathbf{0}, \qquad \text{for DC} \tag{6}$$

$$\frac{\partial}{\partial n} u(\mathbf{r}) = \mathbf{0}, \qquad \text{for NC} \tag{7}$$

where $\partial/\partial n$ denotes the outward normal derivative at $\mathbf{r}$ on S. In (6), $u(\mathbf{r})$ represents E_y while in (7) $u(\mathbf{r})$ represents H_y.

According to our method [9–14], using the current generator Y_{E} and Green's function in random medium $G(\mathbf{r} \mid \mathbf{r}')$, we can express the surface current wave as

$$J(\mathbf{r}_2) = \int_S Y_{\mathrm{E}}(\mathbf{r}_2 \mid \mathbf{r}_1)\, u_{in}(\mathbf{r}_1 \mid \mathbf{r}_i)\, \mathrm{d}\mathbf{r}_1 \tag{8}$$

where $\mathbf{r}_i$ represents the source point location and it is assumed that $\mathbf{r}_i = (0, z)$ in Section 3, and $u_{in}(\mathbf{r}_1 \mid \mathbf{r}_i) = G(\mathbf{r}_1 \mid \mathbf{r}_i)$ whose dimension coefficient is understood. Then, the scattering wave is given by

$$\begin{aligned} u_s(\mathbf{r} \mid \mathbf{r}_i) &= \int_S J_E(\mathbf{r}_2)\, G(\mathbf{r} \mid \mathbf{r}_2)\, \mathrm{d}\mathbf{r}_2, \qquad \text{for E–wave incidence} \\ &= \int_S J_H(\mathbf{r}_2)\, \frac{\partial G(\mathbf{r} \mid \mathbf{r}_2)}{\partial n_2}\, \mathrm{d}\mathbf{r}_2, \quad \text{for H–wave incidence} \end{aligned} \tag{9}$$

that can be expressed as

$$\begin{aligned} u_{\mathrm{s}}(\mathbf{r} \mid \mathbf{r}_i) &= \int_S \mathrm{d}\mathbf{r}_1 \int_S \mathrm{d}\mathbf{r}_2\, [G(\mathbf{r} \mid \mathbf{r}_2) Y_{\mathrm{E}}(\mathbf{r}_2 \mid \mathbf{r}_1) u_{in}(\mathbf{r}_1 \mid \mathbf{r}_{\mathrm{i}})] \\ &\quad \text{for E–wave incidence} \\ &= -\int_S \mathrm{d}\mathbf{r}_1 \int_S \mathrm{d}\mathbf{r}_2 \left[\left(\frac{\partial}{\partial n_2} G(\mathbf{r} \mid \mathbf{r}_2) \right) Y_{\mathrm{H}}(\mathbf{r}_2 \mid \mathbf{r}_1) u_{in}(\mathbf{r}_1 \mid \mathbf{r}_{\mathrm{i}}) \right] \\ &\quad \text{for H–wave incidence} \end{aligned} \tag{10}$$

Therefore, $\langle u_s \rangle$ can be formulated as

$$\begin{aligned} \langle u_{\mathrm{s}}(\mathbf{r} \mid \mathbf{r}_i) \rangle &= \int_S \mathrm{d}\mathbf{r}_1 \int_S \mathrm{d}\mathbf{r}_2\, [Y_{\mathrm{E}}(\mathbf{r}_2 \mid \mathbf{r}_1) \langle G(\mathbf{r}_1 \mid \mathbf{r}_{\mathrm{i}}) G(\mathbf{r} \mid \mathbf{r}_2) \rangle] \\ &\quad \text{for E–wave incidence} \\ &= -\int_S \mathrm{d}\mathbf{r}_1 \int_S \mathrm{d}\mathbf{r}_2 \left[Y_{\mathrm{H}}(\mathbf{r}_2 \mid \mathbf{r}_1) \left\langle \frac{\partial}{\partial n_2} G(\mathbf{r} \mid \mathbf{r}_2) G(\mathbf{r}_1 \mid \mathbf{r}_{\mathrm{i}}) \right\rangle \right] \\ &\quad \text{for H–wave incidence} \end{aligned} \tag{11}$$

Therefore, the average (coherent) intensity of scattered waves for E-wave incidence is given by

$$\begin{aligned} |\langle u_s(\mathbf{r} \,|\, \mathbf{r}_i)\, u_s^*(\mathbf{r}' \,|\, \mathbf{r}_i') \rangle| = & \int_S \mathrm{d}\mathbf{r}_{01} \int_S \mathrm{d}\mathbf{r}_{02} \int_S \mathrm{d}\mathbf{r}_1' \int_S \mathrm{d}\mathbf{r}_2'\, Y_E(\mathbf{r}_{01} \,|\, \mathbf{r}_1') Y_E^*(\mathbf{r}_{02} \,|\, \mathbf{r}_2') \\ & \times \langle G(\mathbf{r}_1' \,|\, \mathbf{r}_i) G(\mathbf{r} \,|\, \mathbf{r}_{01}) G^*(\mathbf{r}_2' \,|\, \mathbf{r}_i') G^*(\mathbf{r}' \,|\, \mathbf{r}_{02}) \rangle \end{aligned} \tag{12}$$

and for H-wave incidence as

$$\begin{aligned} |\langle u_s(\mathbf{r} \,|\, \mathbf{r}_i)\, u_s^*(\mathbf{r}' \mid \mathbf{r}_i') \rangle| = & \int_S \mathrm{d}\mathbf{r}_{01} \int_S \mathrm{d}\mathbf{r}_{02} \int_S \mathrm{d}\mathbf{r}_1' \int_S \mathrm{d}\mathbf{r}_2'\, Y_H(\mathbf{r}_{01} \,|\, \mathbf{r}_1') Y_H^*(\mathbf{r}_{02} \,|\, \mathbf{r}_2') \\ & \times \frac{\partial}{\partial n_{01}} \frac{\partial}{\partial n_{02}} \langle G(\mathbf{r}_1' \,|\, \mathbf{r}_i) G(\mathbf{r} \,|\, \mathbf{r}_{01}) G^*(\mathbf{r}_2' \,|\, \mathbf{r}_i') G^*(\mathbf{r}' \,|\, \mathbf{r}_{02}) \rangle \end{aligned} \tag{13}$$

Here, Y_{E} and Y_{H} are the operator that transforms incident waves into surface currents on S and depends only on the scattering target.

The current generator can be expressed in terms of wavefunctions that satisfy Helmholtz equation and the radiation condition. That is, for E-wave incidence and H-wave incidence, the surface current is obtained as

$$\int_S Y_{\mathrm{E}}(\mathbf{r}_2 \mid \mathbf{r}_1)\, u_{in}(\mathbf{r}_1 \mid \mathbf{r}_i)\, \mathrm{d}\mathbf{r}_1 \simeq \tag{14}$$
$$\mathbf{\Phi}_M^*(\mathbf{r}_2) A_E^{-1} \int_S \ll \mathbf{\Phi}_M^T(\mathbf{r}_1),\, u_{in}(\mathbf{r}_1 \mid \mathbf{r}_i) \gg \mathrm{d}\mathbf{r}_1$$

$$-\int_S Y_{\mathrm{H}}(\mathbf{r}_2 \mid \mathbf{r}_1)\, u_{in}(\mathbf{r}_1 \mid \mathbf{r}_i)\, \mathrm{d}\mathbf{r}_1 \simeq \tag{15}$$
$$-\frac{\partial \mathbf{\Phi}_M^*(\mathbf{r}_2)}{\partial n} A_H^{-1} \int_S \ll \mathbf{\Phi}_M^T(\mathbf{r}_1),\, u_{in}(\mathbf{r}_1 \mid \mathbf{r}_i) \gg \mathrm{d}\mathbf{r}_1$$

where

$$\int_S \ll \mathbf{\Phi}_M^T(\mathbf{r}_1),\, u_{in}(\mathbf{r}_1 \mid \mathbf{r}_i) \gg \mathrm{d}\mathbf{r}_1 \equiv$$
$$\int_S \phi_m(\mathbf{r}_1) \frac{\partial u_{in}(\mathbf{r}_1 \mid \mathbf{r}_i)}{\partial n} - \frac{\partial \phi_m(\mathbf{r}_1)}{\partial n} u_{in}(\mathbf{r}_1 \mid \mathbf{r}_i)\, \mathrm{d}\mathbf{r}_1 \tag{16}$$

Above equation is sometimes called "reaction" named by Rumsey [20]. Here, the basis functions $\mathbf{\Phi}_M$ are called the modal functions and constitute the complete set of wave functions satisfying the Helmholtz equation in free space and the radiation condition; $\mathbf{\Phi}_M = [\phi_{-N}, \phi_{-N+1}, \ldots, \phi_N]$, $M = 2N+1$ is the total mode number, $\phi_m(\mathbf{r}) = H_m^{(1)}(kr)\exp(im\theta)$, and A_E is a positive definite Hermitian matrix given by

$$A_E = \begin{pmatrix} (\phi_1, \phi_1) & \cdots & (\phi_1, \phi_M) \\ \vdots & \ddots & \vdots \\ (\phi_M, \phi_1) & \cdots & (\phi_M, \phi_M) \end{pmatrix} \tag{17}$$

in which its m, n element is the inner product of ϕ_m and ϕ_n:

$$(\phi_m, \phi_n) \equiv \int_S \phi_m(\mathbf{r}) \phi_n^*(\mathbf{r}) \mathrm{d}\mathbf{r} \tag{18}$$

A_H is A_E of (17) with (ϕ_m, ϕ_n) replaced by $(\partial\phi_m/\partial n, \partial\phi_n/\partial n)$. In (15) and (16), $\ll \mathbf{\Phi}_M^T$ denotes the operation (19) of each element of $\mathbf{\Phi}_M^T$ and the function u_{in} to the right of $\mathbf{\Phi}_M^T$

$$\ll \phi_m(\mathbf{r}), u_{in}(\mathbf{r}) \gg \equiv \phi_m(\mathbf{r}) \frac{\partial u_{in}(\mathbf{r})}{\partial n} - \frac{\partial \phi_m(\mathbf{r})}{\partial n} u_{in}(\mathbf{r}) \tag{19}$$

The Y_E and Y_H are proved to converge in the sense of mean on the true operator when $M \to \infty$.

3. ANALYSIS OF RADAR CROSS-SECTION

Here, we derive an analytical form for the fourth moment of Green's function in random medium and, therefore, we will be able to obtain a formula for the backscattered wave intensity. Next, we will use this formula to calculate the RCS of target in random medium.

3.1. Formulation of Backscattering Wave Intensity

In case of backscattered waves, $\mathbf{r} = \mathbf{r}' = \mathbf{r}_i = \mathbf{r}'_i$ and by applying the reciprocity theorem on Green's function, the average intensity of scattered waves for E-wave incidence is given by

$$\begin{aligned}\langle |u_s(\mathbf{r})|^2 \rangle &= \int_S \mathrm{d}\mathbf{r}_{01} \int_S \mathrm{d}\mathbf{r}_{02} \int_S \mathrm{d}\mathbf{r}'_1 \int_S \mathrm{d}\mathbf{r}'_2\, Y_E(\mathbf{r}_{01} \mid \mathbf{r}'_1) Y_E^*(\mathbf{r}_{02} \mid \mathbf{r}'_2) \\ &\quad \times \langle G(\mathbf{r} \mid \mathbf{r}'_1) G(\mathbf{r} \mid \mathbf{r}_{01}) G^*(\mathbf{r} \mid \mathbf{r}'_2) G^*(\mathbf{r} \mid \mathbf{r}_{02}) \rangle \end{aligned} \tag{20}$$

and for H-wave incidence as

$$\begin{aligned}\langle |u_s(\mathbf{r})|^2 \rangle &= \int_S \mathrm{d}\mathbf{r}_{01} \int_S \mathrm{d}\mathbf{r}_{02} \int_S \mathrm{d}\mathbf{r}'_1 \int_S \mathrm{d}\mathbf{r}'_2\, Y_H(\mathbf{r}_{01} \mid \mathbf{r}'_1) Y_H^*(\mathbf{r}_{02} \mid \mathbf{r}'_2) \\ &\quad \times \frac{\partial}{\partial n_{01}} \frac{\partial}{\partial n_{02}} \langle G(\mathbf{r} \mid \mathbf{r}'_1) G(\mathbf{r} \mid \mathbf{r}_{01}) G^*(\mathbf{r} \mid \mathbf{r}'_2) G^*(\mathbf{r} \mid \mathbf{r}_{02}) \rangle \end{aligned} \tag{21}$$

In our representation of $\langle |u_s(\mathbf{r})|^2 \rangle$, we use an approximated solution for the fourth moment of Green's function in random medium M_{22}. Let us assume that the coherence of waves is kept almost complete in propagation of distance $2a$ equals to the mean diameter of the cylinder. This assumption is acceptable in practical cases under the condition (3). On the basis of the assumption, it is important here to point out that we are going to present a quantitative discussion for the numerical results in Section 3. M_{22} can be obtained as the sum of the second moment products [10, 12, 21] on the assumptions that a single point source coincides with a single point observation. That is,

$$\begin{aligned} M_{22} &= \langle G(\mathbf{r} \mid \mathbf{r}'_1) G(\mathbf{r} \mid \mathbf{r}_{01}) G^*(\mathbf{r} \mid \mathbf{r}'_2) G^*(\mathbf{r} \mid \mathbf{r}_{02}) \rangle \\ &\simeq \langle G(\mathbf{r} \mid \mathbf{r}'_1) G^*(\mathbf{r} \mid \mathbf{r}'_2) \rangle \langle G(\mathbf{r} \mid \mathbf{r}_{01}) G^*(\mathbf{r} \mid \mathbf{r}_{02}) \rangle + \\ &\quad \langle G(\mathbf{r} \mid \mathbf{r}'_1) G^*(\mathbf{r} \mid \mathbf{r}_{02}) \rangle \langle G(\mathbf{r} \mid \mathbf{r}_{01}) G^*(\mathbf{r} \mid \mathbf{r}'_2) \rangle \\ &= M_0 \left(M_\alpha + M_\beta \right) \end{aligned} \tag{22}$$

$$\begin{aligned} M_0 &= G_0(\mathbf{r} \mid \mathbf{r}'_1) G_0(\mathbf{r} \mid \mathbf{r}_{01}) G_0^*(\mathbf{r} \mid \mathbf{r}'_2) G_0^*(\mathbf{r} \mid \mathbf{r}_{02}) \\ &= U \exp(X) \end{aligned} \tag{23}$$

$$M_\alpha = \exp(Y_1) \tag{24}$$

$$M_\beta = \exp(Y_2) \tag{25}$$

in which,

$$U = \frac{1}{[8\pi kz]^2} \tag{26}$$

$$X = -jk\,(z_{01} - z_{02} + z_1' - z_2') + \frac{jk}{2(z - z_0)}(x_{01}^2 - x_{02}^2 + x_1^2 - x_2'^2) \tag{27}$$

$$Y_1 = \frac{-k^2}{4}\mu\gamma(z)[(x_{01} - x_{02})^2 + (x_1' - x_2')^2] \tag{28}$$

$$Y_2 = \frac{-k^2}{4}\mu\gamma(z)[(x_{01} - x_2')^2 + (x_1' - x_{02})^2] \tag{29}$$

Here μ and γ are random medium parameters defined as follows:

$$\mu = \sqrt{\pi}\frac{B_0 L^3}{lz^2} \tag{30}$$

$$\begin{aligned}\gamma(z) \;=\; & \frac{2}{(3-n)(2-n)(1-n)}\left(\frac{z}{L}\right)^{3-n} - \frac{n}{1-n}\left(\frac{z}{L}\right)^2 \\ & + \frac{n}{2-n}\left(\frac{z}{L}\right) - \frac{1}{3}\frac{n}{3-n}\end{aligned} \tag{31}$$

Here B_0 is a constant, L is a rough size of the range of the random medium (see Figure 1), and the positive index n denotes the thickness of the transition layer from the random medium to free space; and $n = \frac{8}{3}$ is assumed in Section 3 as in our previous work.

G_0 is the Green's function in free space. We can obtain the RCS by using equations (20) and (21)

$$\sigma = \langle |u_s(\mathbf{r})|^2 \rangle \cdot k(4\pi z)^2 \tag{32}$$

3.2. Numerical Results

Although the incident wave becomes sufficiently incoherent, we should pay attention to the SCL of the incident wave [11–14]. The degree of spatial coherence is defined by

$$\Gamma(\rho, z) = \frac{\langle G(\mathbf{r}_1 \mid \mathbf{r}_t) G^*(\mathbf{r}_2 \mid \mathbf{r}_t)\rangle}{\langle \mid G(\mathbf{r}_0 \mid \mathbf{r}_t) \mid^2 \rangle} \tag{33}$$

where $\mathbf{r}_1 = (\rho, z)$, $\mathbf{r}_2 = (-\rho, z)$, $\mathbf{r}_0 = (0, 0)$, $\mathbf{r}_t = (\rho, 0)$. In the following calculation, we assume $B(\mathbf{r}, \mathbf{r}) = B_0$ and $kB_0 L = 3\pi$; therefore the coherence attenuation index (α) defined as $k^2 B_0 L l/4$

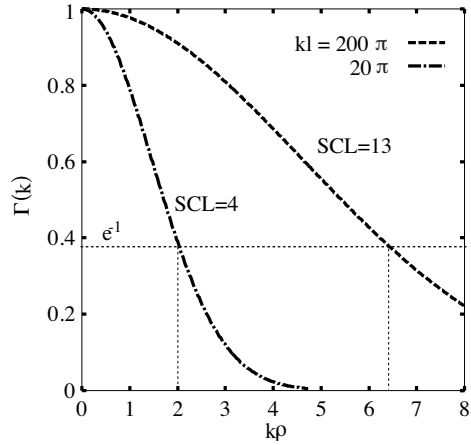

Figure 2. The degree of spatial coherence of an incident wave about the cylinder.

and given in reference [10] is $15\pi^2$ and $150\pi^2$ for $kl = 20\pi, 200\pi$, respectively, which means that the incident wave becomes sufficiently incoherent. The SCL is defined as the $2k\rho$ at which $\mid \Gamma \mid = e^{-1} \simeq 0.37$. Figure 2 shows a relation between SCL and kl in this case and that the SCL is equal to 4, 13. We will use the SCL to represent one of random medium effects on RCS. Under this condition, we may assume that the fourth order moment of Green's functions is expressed as the sum of products of the second order moment.

Here, we point out that N in (17) depends on the target parameters and polarization of incident waves. For example, we choose $N = 24$ at $\delta = 0.1$ for E-wave incidence in the range of $0.1 < ka < 5$; at $ka = 10$, we choose $N = 32$ at $\delta = 0.1$. For H-wave incidence, we choose $N = 28$ at $\delta = 0.1$ in the range of $0.1 < ka < 5$; at $ka = 10$, we choose $N = 40$ at $\delta = 0.1$. As a result, our numerical results are accurate because these values of N lead to convergence of RCS.

Based on the assumption of waves coherence completion in the propagation of distance $2a$, let us define the effective illumination region (EIR) as that surface that is illuminated by the incident wave and restricted by the SCL as shown in Figure 3. Therefore, we expect that the target configuration including δ and ka together with SCL are going to affect the EIR and accordingly the RCS and the enhancement factor of ERCS by a way that will be clarified in Section 3.

In the following, we conduct numerical results for RCS and normalized RCS (NRCS), defined as the ratio of RCS in random media σ to RCS in free space σ_0. Numerical results will be analyzed with a

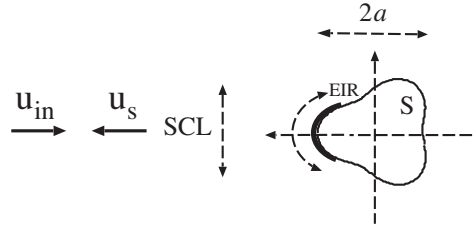

Figure 3. Geometry shows the effective illumination region.

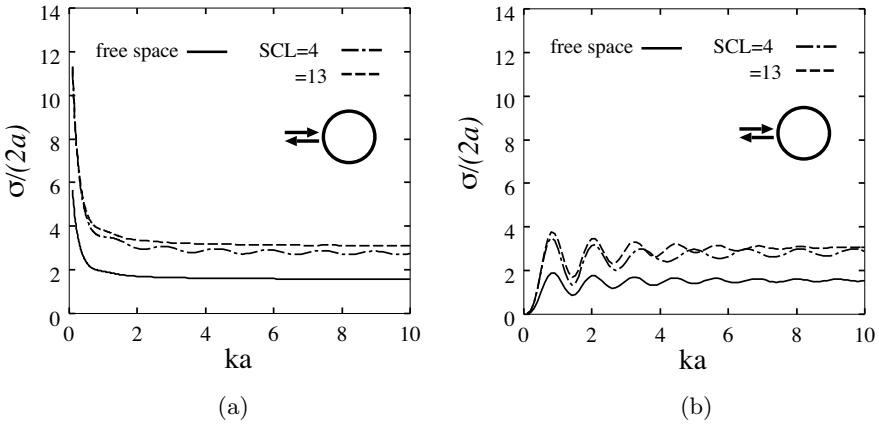

Figure 4. RCS vs. target size in free space and at two different SCLs and $\delta = 0$ where (a) E-wave incidence, (b) H-wave incidence.

variety of parameters including the target in shape and size, angle of incidence, and the wave incidence polarization including E and H-wave incidences. We restrict the shape and size to $\delta = 0$, 0.1, 0.2, 0.3 and $0.1 \leq ka \leq 10$, respectively.

3.2.1. Radar Cross-Section

From the numerical results in Figures 4, 5, and 7, we can notice that there are two factors that affect obviously the RCS. The first is the effect of SCL; as the SCL increases, the behavior of RCS in random media becomes closer to its behavior in free space except for the magnitude of RCS apart from the incident angle and polarization of wave incidence. The second is the effect of target curvature and can be seen clearly with δ and the angle of incidence. Also, we observe that RCS with concave illumination region is larger than that with

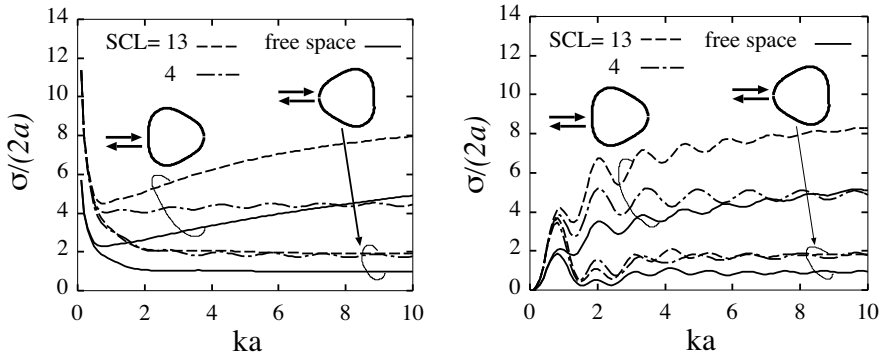

Figure 5. As Figure 4, but for $\delta = 0.1$.

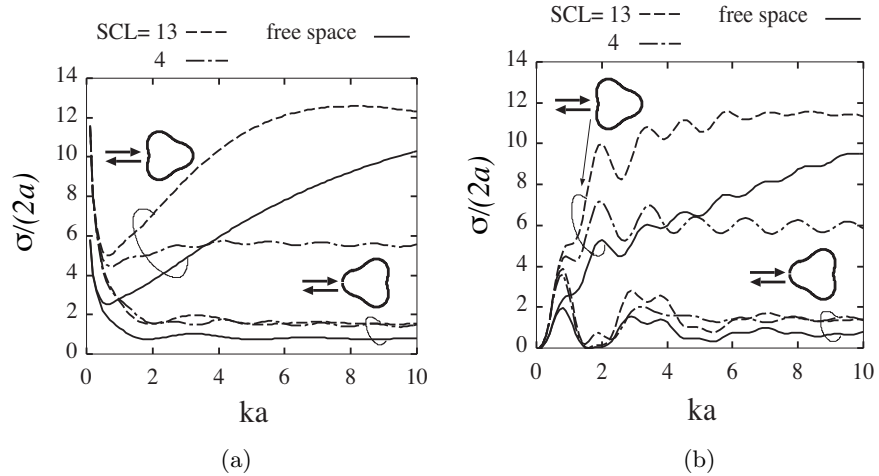

Figure 6. As Figure 4, but for $\delta = 0.2$.

convex illumination region due to the EIR widespread. Furthermore, we can notice an interesting observation, that RCS increases with δ in case of concave illumination region, however, RCS decreases with δ with convex illumination region. This is also attributed to the effect of EIR that can be explained as follows: in case of convex illumination region, as δ increases as the EIR decreases and that leads to a gradual diminishing of RCS; however, for the concave region case, the EIR increases with δ and accordingly the RCS increases. This observation realizes with both E and H-wave incidences.

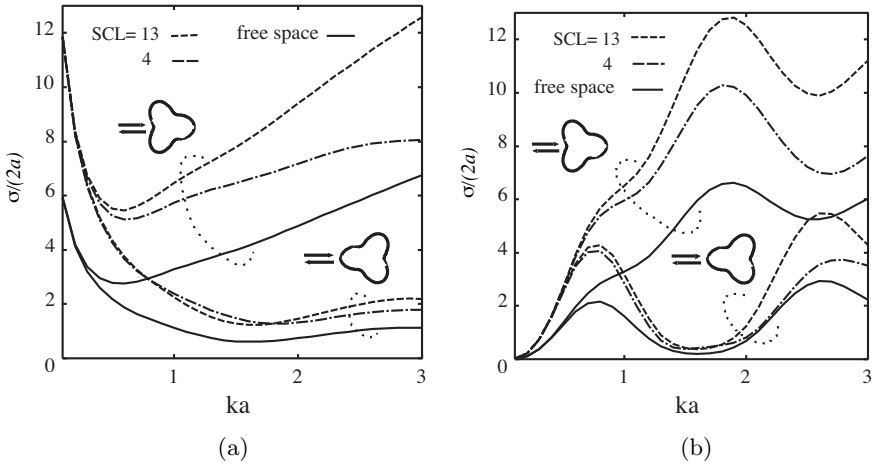

Figure 7. As Figure 4, but for $\delta = 0.3$.

In case of H-wave incidence, RCS undergoes oscillated behavior in both cases of free space and random medium. For free space case, the oscillated behavior, here, that is absent in case of E-wave incidence is due, as a matter of fact, to the effect of creeping waves [22]. At the point of tangency, each wave creeps around the surface at a velocity less than that in free space and that is attenuated by tangential radiation. For low ka values, wave can continue to creep around the target many times and, therefore, the interference between the specularly reflected and creeping waves is obvious enough to affect the RCS resulting in that oscillated behavior. However, with larger ka, the creeping waves travel along the cylinder and they become weaker and weaker the farther they have to travel due to radiation. Therefore the creeping waves attenuation reduces its effectiveness rapidly resulting in diminishing the interference effect gradually with ka. For random medium case, the oscillation is attributed to the effect of creeping waves propagating in random medium that in turn has another effect on the RCS as has been pointed out in our papers.

3.2.2. Backscattering Enhancement

To investigate the ERCS, we conduct numerical results for NRCS for both cases of E and H-wave incidences, results are shown in Figures 8 and 9. From these figures, we note clearly an important observations that characterize wave scattering from partially convex targets in random media. That is the difference in the behavior of the NRCS between both of concave and convex illumination portions apart from

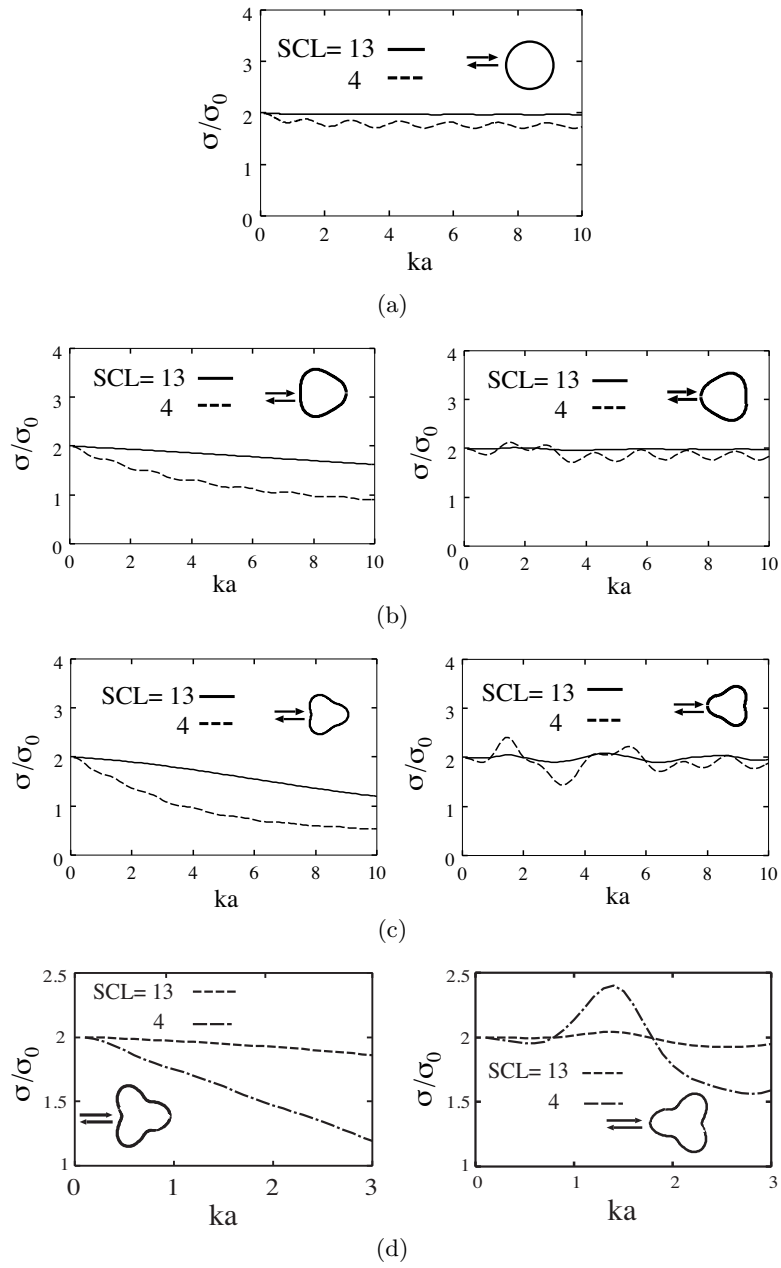

Figure 8. Normalized RCS vs. target size at two different incident angles and SCLs for E-wave incidence where (a) $\delta = 0$, (b) $\delta = 0.1$, (c) $\delta = 0.2$, (d) $\delta = 0.3$ and σ, σ_0 are RCS in random media and in free space, respectively.

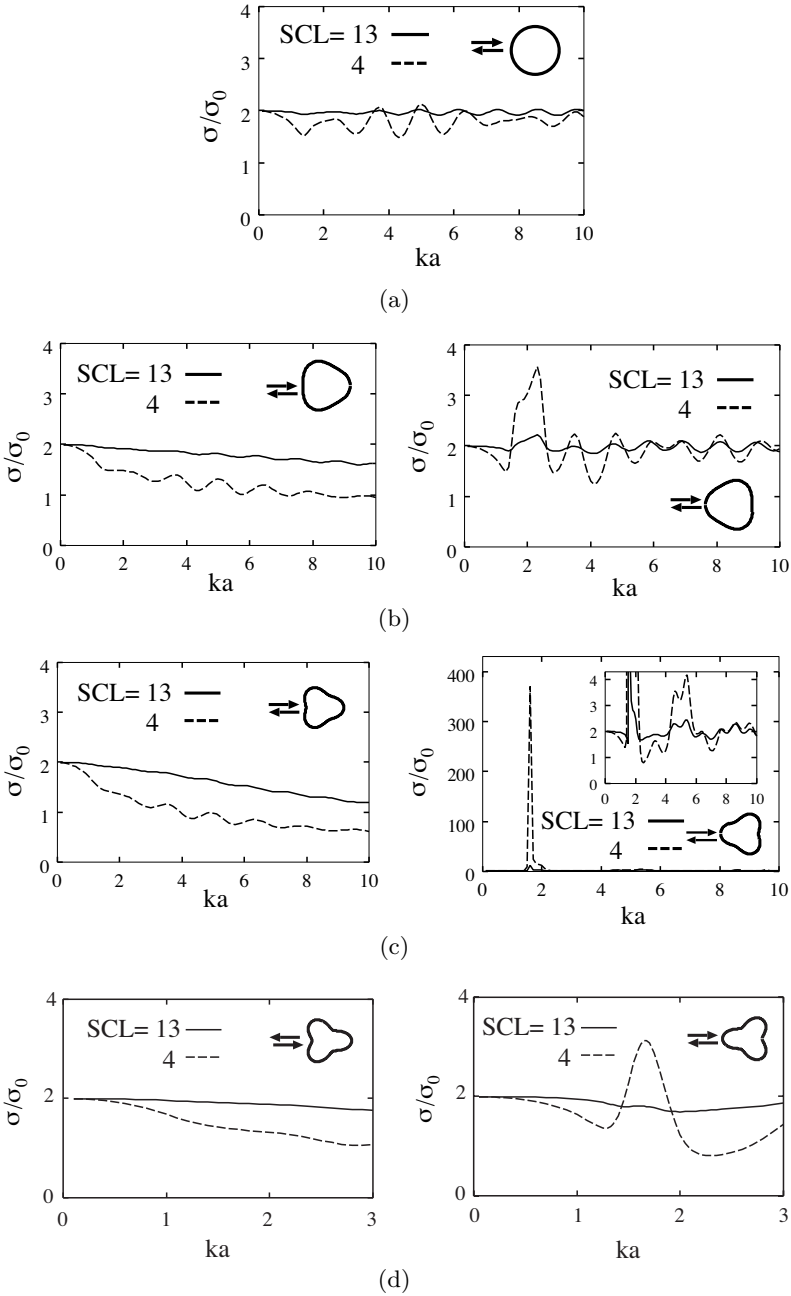

Figure 9. As Figure 8, but for H-wave incidence.

the incidence wave polarization as a result of the EIR effect as explained previously. In fact, owing to the double passage effect, NRCS equals two [1]; this fact holds when SCL $\gg ka$ irrespective also of the incident waves polarization as shown in Figures 8 and 9. However, NRCS deviates from this value with increasing ka and/or δ; this deviation in NRCS decreases with the increase in SCL. For concave illumination portion, NRCS decreases gradually with some fluctuations for H-wave incidence as a result of the difference in the creeping waves effects between both of free space and random media. On the other hand, for convex illumination portion, NRCS fluctuates slowly around two; this fluctuation increases with δ. This analysis demonstrates clearly the effect of the illumination portion curvature in conjunction with SCL of incident waves on NRCS.

Also, we observe the dramatic increase in NRCS when SCL = 4, $ka = 1.6$, and $\delta = 0.2$ as shown in Figure 9(c). This enhancement occurs strongly for H-wave incidence on convex portion; detailed study of this strong enhancement is presented in [12, 13].

4. ANALYSIS OF ANGULAR CORRELATION FUNCTION

In this section, we derive an analytical form for the fourth moment of Green's function in random medium and, therefore, we will be able to obtain a formula for the scattered wave intensity. Next, we will use this formula to calculate the angular correlation function (ACF) of target in random medium.

4.1. Problem Formulation

Let us assume that source and observation points are on the same circle of r. Then $u_s(\mathbf{r})$ is expressed as $u(\theta_{i1}, \theta_{r1})$ and represents the scattered wave observed at the scattering angle θ_{r1} when the incident angle is θ_{i1}. Suppose that the incident angle is changed from θ_{i1} to θ_{i2} and the scattered wave $u(\theta_{i2}, \theta_{r2})$ is observed at θ_{r2} (see Figure 10) . The angular correlation function (ACF) Γ can be obtained from equations (12) and (13), Γ is defined in terms of incident and scattered angles as

$$\Gamma(\theta_{i1}, \theta_{i2}, \theta_{r1}, \theta_{r2}) = \langle u_s(\theta_{i1}, \theta_{r1})\, u_s^*(\theta_{i2}, \theta_{r2}) \rangle \tag{34}$$

where $\theta_{r1} = \theta_{i1} + \psi$, $\theta_{i2} = \theta_{i1} + \theta_1$, $\theta_{r2} = \theta_{r1} + \theta_2$, and θ_1 and θ_2 are the deviation in both angles of reference incident and scattered waves.

Under the condition that incident and scattered waves are not correlated, we may assume that the fourth order moment of Green's

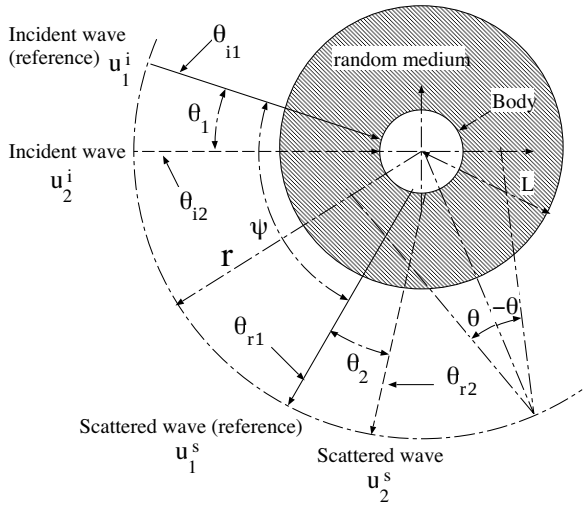

Figure 10. Angular correlation of waves scattered by a conducting cylinder in a random medium.

functions is expressed as the product of the second order moments as follows.

$$\begin{aligned} M_{22} &= \langle G(\mathbf{r} \mid \mathbf{r}_{01}) G(\mathbf{r}_1' \mid \mathbf{r}_i) G^*(\mathbf{r}' \mid \mathbf{r}_{02}) G^*(\mathbf{r}_2' \mid \mathbf{r}_i') \rangle \\ &\simeq \langle G(\mathbf{r} \mid \mathbf{r}_{01}) G^*(\mathbf{r}' \mid \mathbf{r}_{02}) \rangle \langle G(\mathbf{r}_1' \mid \mathbf{r}_i) G^*(\mathbf{r}_2' \mid \mathbf{r}_i') \rangle \\ &= M_0 \, M_\alpha \end{aligned} \tag{35}$$

$$\begin{aligned} M_0 &= G_0(\mathbf{r} \mid \mathbf{r}_{01}) G_0(\mathbf{r}_1' \mid \mathbf{r}_i) G_0^*(\mathbf{r}' \mid \mathbf{r}_{02}) G_0^*(\mathbf{r}_2' \mid \mathbf{r}_i') \\ &= U \exp(R) \end{aligned} \tag{36}$$

$$M_\alpha = \exp(W) \tag{37}$$

$$\begin{aligned} R &= -jk\,(z_{01} - z_{02} + z_1' - z_2') \\ &\quad + \frac{jk}{2(z - z_0)} \{ (\rho_i + \rho_i' - \rho_1' - \rho_2')(\rho_i - \rho_i' - \rho_1' + \rho_2') \\ &\quad (\rho_r + \rho_r' - \rho_{01} - \rho_{02})(\rho_r - \rho_r' - \rho_{01} + \rho_{02}) \} \end{aligned} \tag{38}$$

$$\begin{aligned} W &= \frac{-k^2}{4} \mu \Big\{ \alpha(z, z_0)[(\rho_i - \rho_i')^2 + (\rho_r - \rho_r')^2] \\ &\quad + \beta(z, z_0)[(\rho_t - \rho_i')(\rho_1' - \rho_2') + (\rho_r - \rho_r')(\rho_{01} - \rho_{02})] \\ &\quad + \gamma(z, z_0)[(\rho_1' - \rho_2')^2 + (\rho_{01} - \rho_2')^2] \Big\} \end{aligned} \tag{39}$$

where

$$\alpha(z,z_0) = \frac{1}{3-n}\left(\frac{z}{L}\right)^{3-n} - \frac{2}{2-n}\left(\frac{z_0}{L}\right)\left(\frac{z}{L}\right)^{2-n} + \frac{1}{1-n}\left(\frac{z_0}{L}\right)^2\left(\frac{z}{L}\right)^{1-n} - \frac{n}{3(3-n)} + \frac{2}{2-n}\left(\frac{z_0}{L}\right) - \frac{1}{1-n}\left(\frac{z_0}{L}\right)^2 - \frac{1}{3}\left(\frac{z_0}{L}\right)^3 \quad (40)$$

$$\beta(z,z_0) = \frac{2}{(3-n)(2-n)}\left(\frac{z}{L}\right)^{3-n} - \frac{2}{(2-n)(1-n)}\left(\frac{z_0}{L}\right)\left(\frac{z}{L}\right)^{2-n} + \left[\left(\frac{z_0}{L}\right)^2 + \frac{2n}{1-n}\left(\frac{z_0}{L}\right)^2 - \frac{n}{2-n}\right]\left(\frac{z}{L}\right) + \frac{2}{3}\frac{n}{3-n} - \frac{n}{2-n}\left(\frac{z_0}{L}\right) - \frac{1}{3}\left(\frac{z_0}{L}\right)^3 \quad (41)$$

μ, γ are defined in equations (30) and (31), $z_0 = a$.

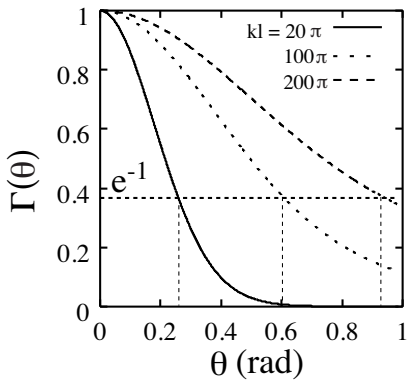

Figure 11. The degree of spatial coherence of an incident wave about the cylinder.

4.2. Numerical Results

The degree of spatial coherence is expressed as a function of θ on the circle of radius r, shown in Figure 11, and can be defined by

$$\Gamma(\theta) = \frac{\langle G(\theta \mid 0) G^*(-\theta \mid 0)\rangle}{\langle \mid G(0 \mid 0) \mid^2 \rangle} \quad (42)$$

The SCL is defined as $2k\rho$ at which $k\rho = kr\sin\theta$ where θ is defined as $\mid \Gamma(\theta) \mid = e^{-1} \simeq 0.37$ in Figure 11 where $kr = 6$ for convenience.

Accordingly, in this case SCL is approximately equal to 3.2, 6.8, and 9.5, for $kl = 20\pi$, 100π, 200π, respectively.

The correlation function of the scattered waves defined by equation (34) was calculated numerically as a function of the following parameters.

- Target shape: we handle different target shapes including circular, elliptic, and concave-convex surfaces. Also we will change the parameters of the different shapes. For elliptic cylinders we will change the axis ratio (b/a) where b and a are defined in equation (4). For the concave-convex targets we will change δ defined in equation (5).
- Target size: We will deal with different sizes for targets by changing ka.
- Incident angle: Different incident angles will be handled by changing ϕ.
- Incident wave polarization: E and H-wave incidences.
- Random medium parameter kl.

In our numerical results we will postulate θ_{i1} and ψ to equal 0.98π and 0.04 [rad], respectively, to keep the assumption that incident and scattered waves are not correlated. In Figures 12 to 15 we present numerical results for ACF for E-wave incidence on targets of different shapes where $ka = 1$, $\phi = 0$, and $kl = 20\pi$. From Figures 12 to 15 we observe that ACF doesn't change with shape of target. Afterwards we proceed in our study; in Figures 16 to 21 we change ka, ϕ, polarization, and kl, respectively, compared to previous case of Figures 12 to 15.

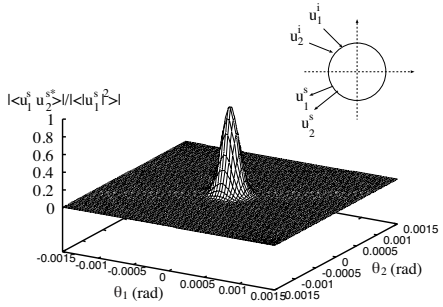

Figure 12. Normalized angular correlation function for convex cylinder where $b/a = 1$ and for E-wave incidence.

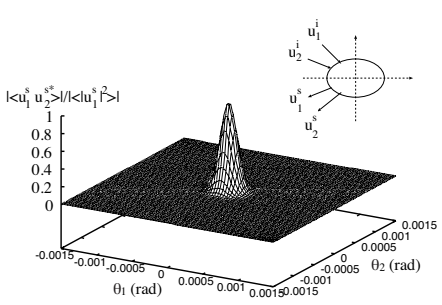

Figure 13. As Fig. 12, but for $b/a = 0.6$.

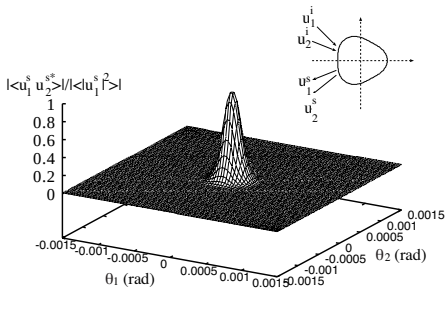

Figure 14. Normalized angular correlation function for concave-convex cylinder where $\delta = 0.1$.

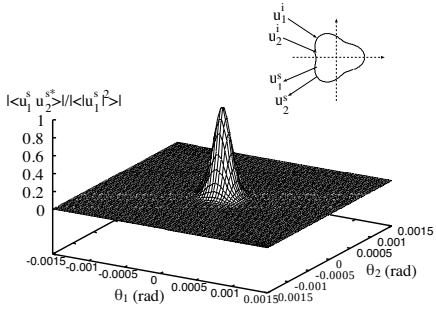

Figure 15. As Fig. 14, but for $\delta = 0.2$.

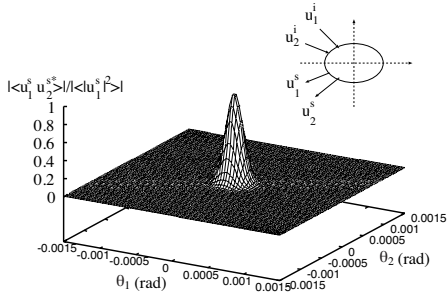

Figure 16. As Fig.13, but for $ka = 3$.

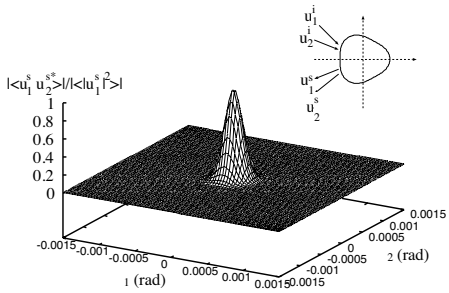

Figure 17. As Fig. 14, but for $ka = 2$.

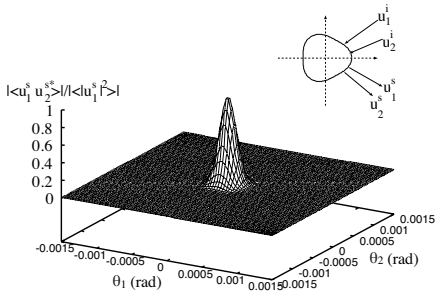

Figure 18. As Fig. 14, but for $\phi = \pi$.

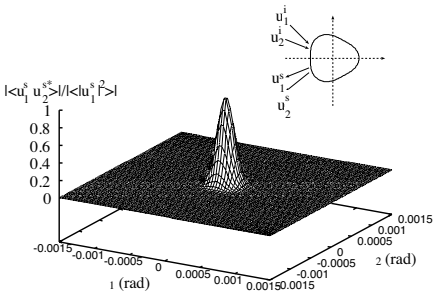

Figure 19. As Fig. 14, but for H-wave incidence.

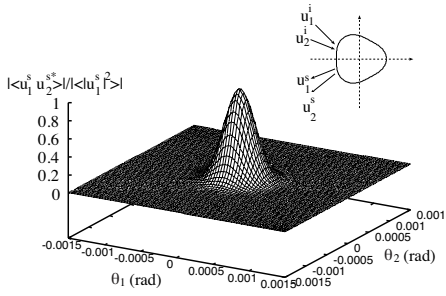

Figure 20. As Fig. 14, but for $kl = 60\pi$.

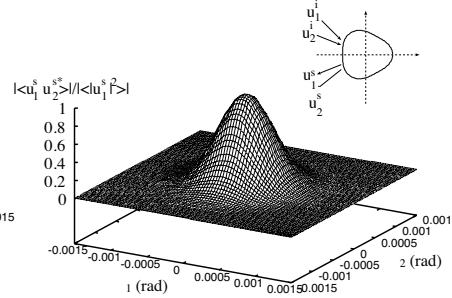

Figure 21. As Fig. 14, but for $kl = 200\pi$.

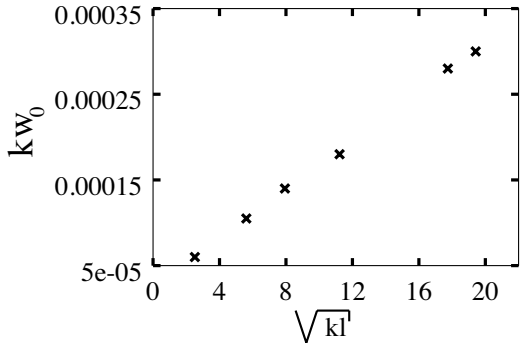

Figure 22. Relationship between scale size and correlation width of the scattered waves from circular cylinder in random medium.

From Figures 16 to 21, we observe that ACF does not change with target size, incident wave angle, and polarization.

The ACF changes obviously with the random media. As kl increases, the SCL increases too as shown in Figure 2 and also there is another increase in the correlation width w defined as $2k\rho$ at which $\rho = r\sin\theta$ where θ is defined as the angle at which ACF$= e^{-1} \simeq 0.37$. In Figure 22 we draw a relationship between the square root of kl and w where a circular cylinder of $ka = 1$ is assumed; it is clear that w is almost directly proportional to the square root of kl. This fact shows also that the ACF depends on the random media.

Also ACF changes with incident angle and to clarify such change, we plotted ACF in two-dimensional graph as shown in Figure 23. It is clear that as increasing θ_1 slightly the ACF decreases obviously which reveals that ACF is very sensitive to the incident angle deviation.

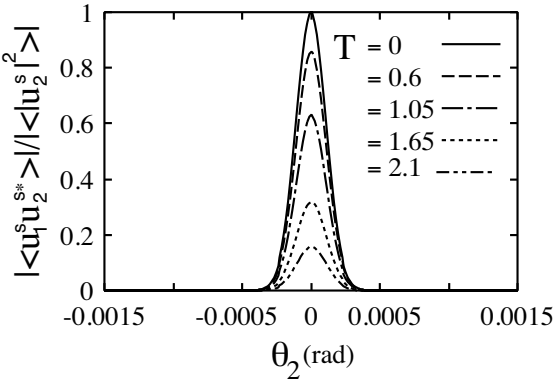

Figure 23. Clarification of angular correlation function at $kl = 20\pi$; $\theta_1 = T * 10^{-4}\,[rad]$.

5. CONCLUSION

We have considered the scattering problems of plane waves incidence on targets in free space and random media. Using the method that assumes a current generator together with Green's function we obtained a formulation for the scattering waves from targets in random media. Next, we have investigated numerically the RCS, the backscattering enhancement, and the angular correlation function (ACF) of scattering waves from conducting concave-convex targets with the SCL, incident wave polarization, and target parameters.

In addition to the well-known effect of the double passage of waves in random media, we have demonstrated the clear effects of target configuration together with the SCL on the RCS and backscattering enhancement. These characteristics realize apart from the incident angle and the incident wave polarization.

Numerical results suggest an important fact; the ACF depends only on the random media irrespective of targets parameters and incident wave polarization on the assumption that incident and scattered waves are not correlated. As a result, we could find that the correlation width of the ACF is directly proportional to the square root of scale-size of random media.

ACKNOWLEDGMENT

This work was supported in part by the National Science and Engineering Research Councial of Canada under grant 250299-02.

REFERENCES

1. Kravtsov, Yu. A. and A. I. Saishev, "Effects of double passage of waves in randomly inhomogeneous media," *Sov. Phys. Usp.*, Vol. 25, 494–508, 1982.
2. Jakeman, E., "Enhanced backscattering through a deep random phase screen," *J. Opt. Soc. Am.*, Vol. 5, No. 10, 1638–1648, 1988.
3. Welch, G. and R. Phillips, "Simulation of enhanced backscattered by a phase screen," *J. Opt. Soc. Am.*, Vol. 7, No. 4, 578–584, 1990.
4. Ishimaru, A., "Backscattering enhancement: from radar cross sections to electron and light localizations to rough surface scattering," *IEEE Antennas and Propagation Magazine*, Vol. 33, No. 5, 1–7, 1991.
5. Mishchenko, M. I., "Enhanced backscattering of polarized light from discrete random media: calculation in exactly the backscattering direction," *J. Opt. Soc. Am.*, Vol. 9, No. 6, 978–982, 1992.
6. Keller, J. B. and W. Streifer, "Complex rays with an application to Gaussian beams," *J. Opt. Soc. Am.*, Vol. 61, No. 1, 40–43, 1971.
7. Ikuno, H., "Calculation of far-scattered fields by the method of stationary phase," *IEEE Transactions on Antennas and Propagation*, Vol. AP-27, No. 2, 199–202, 1979.
8. Bennett, C. L. and Mieras, "Time domain scattering from open thin conducting surfaces," *Radio Science*, Vol. 16, No. 6, 1231–1239, 1981.
9. Tateiba, M. and E. Tomita, "Theory of scalar wave scattering from a conducting target in random media," *IEICE Trans. Electron.*, Vol. E75-C, No. 1, 101–106, 1992.
10. Tateiba, M. and Z. Q. Meng, "Wave scattering from conducting bodies in random media — theory and numerical results," *Electromagnetic Scattering by Rough Surfaces and Random Media*, M. Tateiba and L. Tsang (eds.), PIER 14, 317–361, PMW Pub., Cambridge, MA, USA, 1996.
11. Meng, Z. Q. and M. Tateiba, "Radar cross sections of conducting elliptic cylinders embedded in strong continuous random media," *Waves in Random Media*, Vol. 6, 335–45, 1996.

12. El-Ocla, H. and M. Tateiba, "Strong backscattering enhancement for partially convex targets in random media," *Waves in Random Media*, Vol. 11, No. 1, 21–32, 2001.
13. El-Ocla, H. and M. Tateiba, "Analysis of backscattering enhancement for complex targets in continuous random media for H-wave incidence," *IEICE Trans. Commun.*, Vol. E84-B, No. 9, 2583–2588, 2001.
14. El-Ocla, H. and M. Tateiba, "Backscattering enhancement for partially convex targets of large sizes in continuous random media for E-wave incidence," *Waves in Random Media*, Vol. 12, No. 3, 387–397, 2002.
15. Michel, T. R. and K. A. O'Donnell, "Angular correlation function of amplitudes scattered from a one-dimensional perfectly conducting rough surface," *J. Opt. Soc. Am.*, Vol. 9, No. 8, 1374–1384, 1992.
16. Le, C. T. C., Y. Kuga, and A. Ishimaru, "Angular correlation function based on the second-order Kirchhoff approximation and comparison with experiments," *J. Opt. Soc. of America*, Vol. 13, No. 5, 1057–1067, 1996.
17. Chan, T.-K., Y. Kuga, and A. Ishimaru, "Subsurface detection of a buried object using angular correlation function measurement," *Waves in Random Media*, Vol. 7, 457–465, 1997.
18. Tateiba, M. and Y. Nagatake, "Scattered waves from a conducting cylinder embedded in a random medium," *Proc. International Geoscience and Remote Sensing*, Vol. 1, 45–47, 1998.
19. Ishimaru, A., *Wave Propagation and Scattering in Random Media*, IEEE press, 1997.
20. Rumsey, V. H., "Reaction concept in electromagnetic theory," *Physical Review*, Vol. 94, 1483–1491, 1954.
21. Dashen, R., "Path integrals for waves in random media," *J. Math. Phys.*, Vol. 20, No. 5, 894–920, 1979.
22. Harbold, M. L. and B. N. Steinberg, "Direct experimental verification of creeping waves," *The Journal of the Acoustical Society of America*, Vol. 45, 592–603, 1969.